

Electronic Supplementary Information (ESI)

Preparation of $\text{YbF}_3\text{-Ho@TiO}_2$ core-shell sub-microcrystal spheres and their application to the electrode of dye-sensitized solar cells

Jia Yu,^{a,b,c*} Yulin Yang,^{d,*} Chuanxiang Zhang,^{b,e*} Ruiqing Fan,^d Ting Su^f

^a Hami Vocational & Technical College, Hami, 839000, P. R. China.

^b Henan Key Laboratory of Coal Green Conversion, College of Chemistry and Chemical Engineering, Henan Polytechnic University, Jiaozuo, 454003, P. R. China.

^c Hami Yuxin Energy Industry Research Institute Co., Ltd., 839000, P. R. China.

^d MIIT Key Laboratory of Critical Materials Technology for New Energy Conversion and Storage, School of Chemistry and Chemical Engineering, Harbin Institute of Technology, Harbin 150001, P. R. China.

^e Collaborative Innovation Center of Coal Work Safety, Jiaozuo, 454003, P. R. China.

^f Green Chemistry Centre, College of Chemistry and Chemical Engineering, Yantai University, Yantai 264005, P. R. China.

Corresponding Authors E-mail addresses:

yujiade1987@126.com; ylyang@hit.edu.cn and zcx223@hpu.edu.cn.

SUPPLEMENT

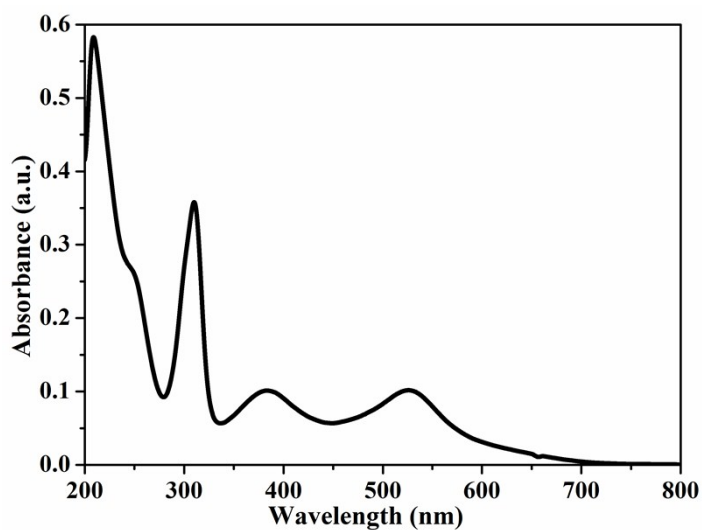


Fig. S1 The absorbance spectrum of N719 dye in ethylalcohol.

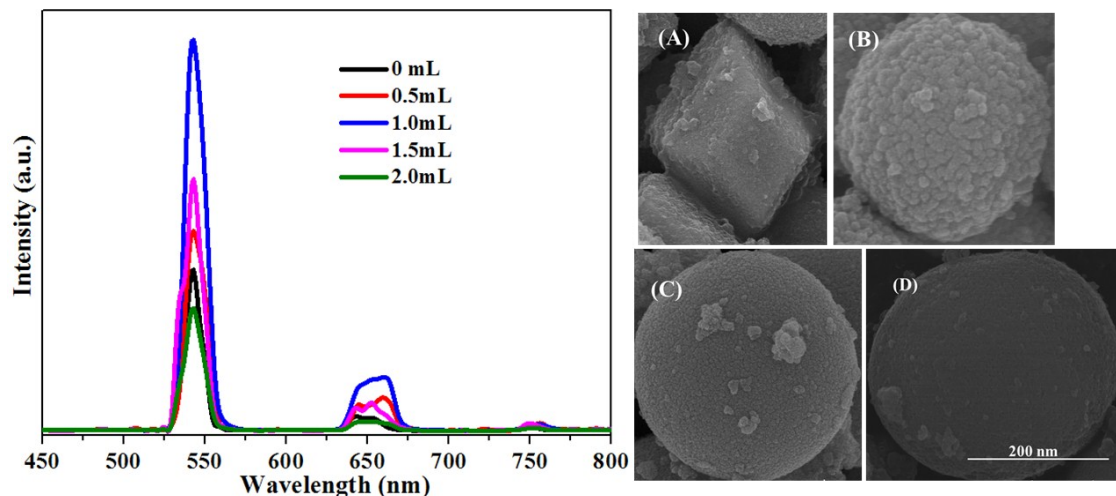


Fig. S2 Upconversion emission spectra of $\text{YbF}_3\text{-Ho@TiO}_2$ with different amount of titanium isopropylate in the synthesis process and the inset are their corresponding SEM images (A) 0.5 mL, (B) 1mL, (C) 1.5 mL and (D) 2 mL.

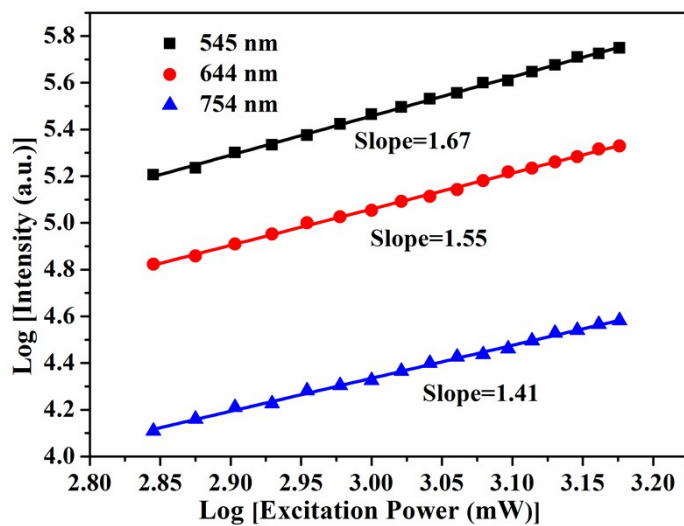


Fig. S3 The upconversion emission intensity as a function of excitation power from a 980 nm laser at 545 nm, 644nm and 754 nm for $\text{YbF}_3\text{-Ho@TiO}_2$.

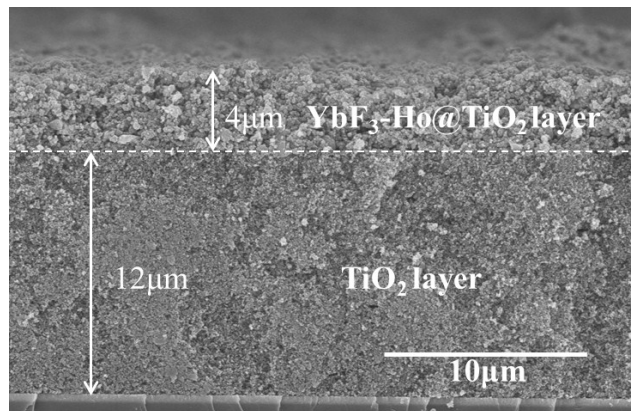


Fig. S4 Cross-section SEM image of $\text{TiO}_2/\text{YbF}_3\text{-Ho@TiO}_2$ heterostructured photoanode film.

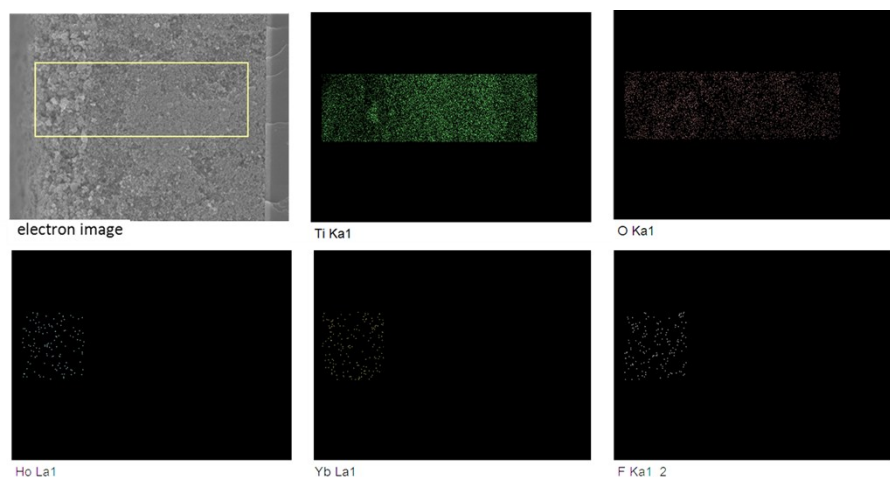


Fig. S5 Element mapping of the cross-section $\text{TiO}_2/\text{YbF}_3\text{-Ho@TiO}_2$ heterostructured photoanode film.

photoanode film.

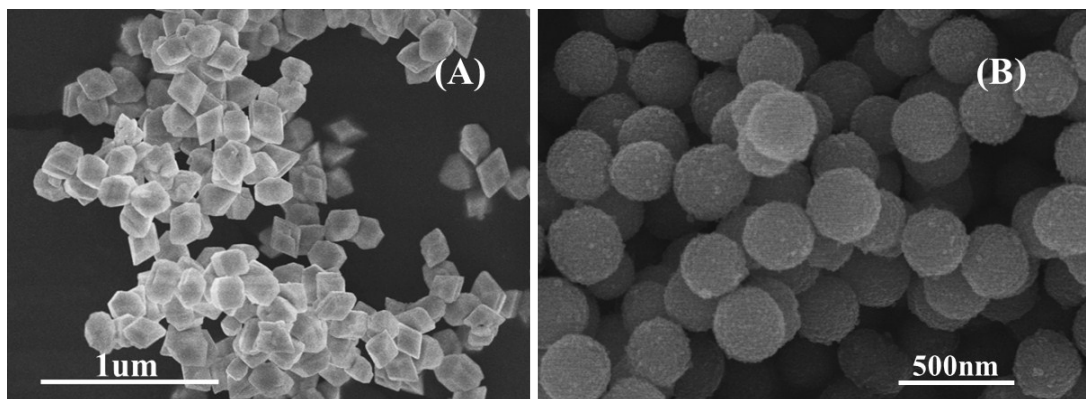


Fig. S6 SEM images of (A) YbF₃ and (B) YbF₃@TiO₂.

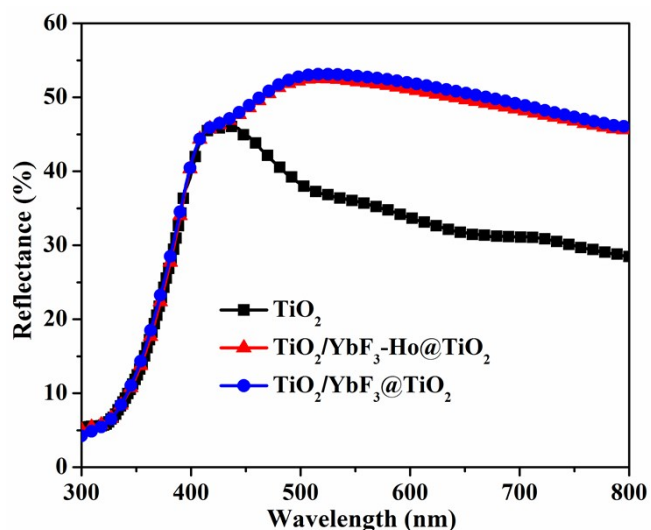


Fig. S7 Diffused reflectance spectra of different photoanode films.

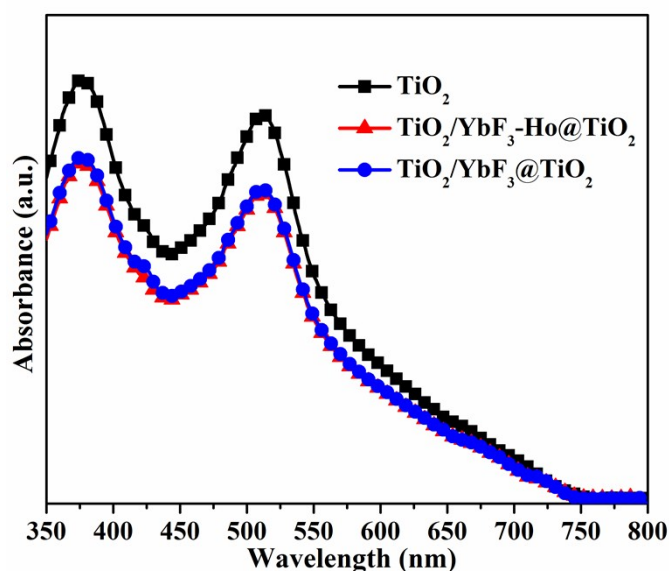


Fig. S8 UV-vis spectra of desorbed dye solutions from sensitized photoanodes.

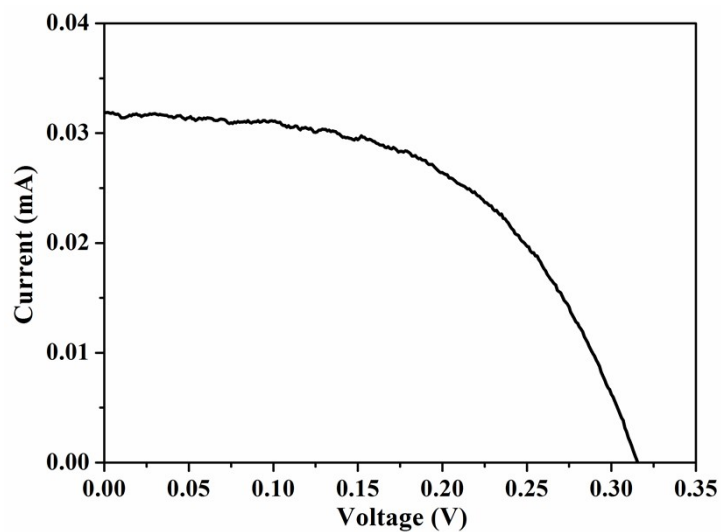


Fig. S9 Photocurrent-voltage curve of DSSC with $\text{TiO}_2/\text{YbF}_3\text{-Ho@TiO}_2$ under 980 nm laser illumination.

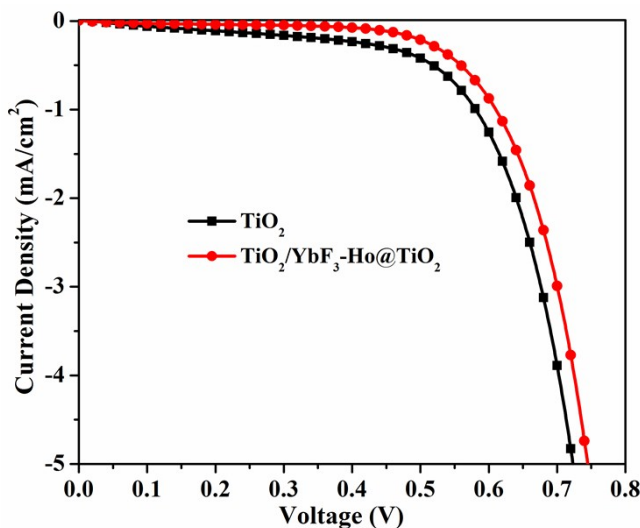


Fig. S10 Dark current-voltage curves of DSSCs assembled with TiO_2 and $\text{TiO}_2/\text{YbF}_3\text{-Ho@TiO}_2$ photoanodes.